Nuclear Engineering and Design 383 (2021) 111386

Contents lists available at ScienceDirect

Nuclear Engineering and Design

journal homepage: www.elsevier.com/locate/nucengdes

A correlation for pool entrainment phenomenon

M. Ouallal [a,*], S. Leyer [a], S. Gupta [b]

[a] Faculty of Science, Technology and Communication, University of Luxembourg, Campus Kirchberg, Luxembourg L-1359, Luxembourg
[b] Becker Technologies GmbH, Rahmann Straße 11, 65760 Eschborn, Germany

ARTICLE INFO

Keywords:
Entrainment
Superficial gas velocity
Droplets
Flow regimes

ABSTRACT

The present work aims to study the phenomena of droplet entrainment from water pool in a confined atmosphere, which could be either a consequence of boiling or depressurization. Eventually, these droplets are entrained by the streaming gas (superficial gas velocity) or settling down due to gravity.

The number of correlations developed so far quantify the entrainment based on empirical, semi-empirical and theoretical approaches, but they have been generally limited to a specific flow-regime in the water pool, thermal hydraulic conditions or even to a specific geometry. In this context, the present work aims to develop an empirical correlation to cover the flow regimes from bubbly to churn turbulent, and could be applied to a wide range of geometries. The present correlation shows an increase until a maximum entrainment of about 2.10^{-4}, corresponding to superficial gas velocity of 0.05 m/s for bubbly flow regime, and then a slight decrease to $2{\cdot}10^{-5}$, for the transition regime corresponding superficial gas velocity of 0.1 m/s, and a sharp increase in the churn turbulent flow regime as the gas velocity goes up to 5 m/s.

The experimental database used to develop the present empirical correlation covers a broader range of boundary conditions, namely pressure [1 bar–15 bar], water pool thermal condition [subcooled – boiling], vessel diameter [0.19 m- 3.2 m], pool diameter [0.1 m–1.4 m], superficial gas velocity up to 5.0 m/s Therefore, the proposed empirical correlation aims to constitute an important tool to transfer the experimental results to reactor application.

1. Introduction

The entrainment of liquid phase by a gas phase is found in a numerous industrial process, where mass and heat transfer intervene. During the interaction liquid–gas, the formation of the droplets is a common phenomenon. Taking their size into account, and the exchange with the gas phase, they can be entrained by this latter to a specific height above the water surface. The superficial gas velocity characterizes the gas phase.

The superficial gas velocity is calculated from the volume flow rate of the gas coming from the pool surface of a certain cross section area. Therefore, for different superficial gas velocities comes different flow regimes in the water pool. At low superficial gas velocities, the regime is attributed to a bubbly flow, where bubble are defined in shapes and size. This flow regime is composed of two flow regimes, a homogeneous flow regime where bubble could be assumed to be uniform in size, and heterogeneous flow regime where bubble follow a size distribution (Shah et al., 1982). At high superficial gas velocities, where the irregular shapeless bubble are formed, the regime is attributed to churn turbulent flow. As a function of the flow regimes, the droplet generation mechanism differs from bubble burst to detachment from liquid ligaments due to momentum exchange between gas–liquid (Fig. I-1). The present study concerns the release of these droplets, or so-called droplet entrainment from water pool covering both bubbly flow and churn turbulent flow regimes.

The phenomenon of entrainment is found in industrial processes as well as in natural phenomena, viz. from geophysics (release of salt from the surface of the sea), water treatment (desalination) to nuclear applications (release of aerosol from water pool).

In natural phenomena, the entrainment is responsible for the liquid side mass transfer at the surface of the sea. Sea spray, which is the amount of droplets generated either from bubble burst or roll wave or by splashing containing salts and bacteria from the sea surface (Blanchard, 1989; Spiel, 1998a; Spiel, 1998b) are entrained by the wind and could be problematic for human health as it could affect the climate. The released aerosol might form large clouds that could affect the air quality as well as reflecting the sun light. The weather in coastal region is mainly

* Corresponding author.
E-mail addresses: mohammedouallal2@gmail.com, mohammed.ouallal.002@student.uni.lu (M. Ouallal), stephan.leyer@uni.lu (S. Leyer), gupta@becker-technologies.com (S. Gupta).

https://doi.org/10.1016/j.nucengdes.2021.111386
Received 7 April 2021; Received in revised form 19 July 2021; Accepted 21 July 2021
Available online 14 August 2021
0029-5493/© 2021 Elsevier B.V. All rights reserved.

Nomenclature

Acronyms

ALPHA	Assessment of Loads and Performance of Containment in a Hypothetical Accident
BWR	Boiling water reactor
CFD	Computational Fluid Dynamics
LOCA	Loss of Cooling Accident
PWR	Pressurized Water Reactor
REST	REsuspension Source Term
REVENT	REentraiment by VENTing
THAI	Thermal-hydraulic Hydrogen Aerosol Iodine

Nomenclature

A	Vessel cross section$[m^2]$
a	Capillary length$[m]$
a'	Correlation constant equation
C_K	Constant of Kruzhilin correlation.
b'	Correlation constant
d_b	Bubble diameter$[m]$
$d_{b,crit}$	Critical bubble diameter$[m]$
D_H	Vessel diameter$[m]$
d_{dr}	Droplet diameter$[m]$
D_P	Diameter of Pool$[m]$
E_{fg}	Liquid entrainment$[-]$
$f(d)$	Bubble size distribution
$F(d_{dr,crit})$	Fraction of ejected droplets less than$d_{dr,crit}$
f	Correlation constant equation (9) Chapter 2
g	Acceleration due to gravity$[m.s^{-2}]$
h	Height above the water surface in the case of bubbling$[m]$
h_{film}	Bubble film thickness$[m]$
j_g	Superficial gas velocity$[m.s^{-1}]$
j_t	Transition gas velocity$[m.s^{-1}]$
j	Correlation constant equation
k_i, with$i = 1\cdots5$,	Correlation constant of Cosandey's correlation
N_{dr}	Number of jet droplets produced by a single bubble
P_i	Pressure inside the bubble$[bar]$
P_o	Pressure of the surrounding$[bar]$
R_0	Radius of the bubble$[m]$
S_f	Acceleration inside the bubble due to centripetal force$[m.s^{-2}]$
t	Time$[s]$
v_t	Droplet terminal velocity$[m.s^{-1}]$
V_{dr}	Total volume of liquid droplet per volume bubble$V_b[m^3]$
$\dot{V}_{dr}$	Droplets volume flow rate$[m^3.s^{-1}]$
V_b	Bubble volume$[m^3]$
V_{tc}	The roll film velocity (Taylor – Culick velocity)$[m/s]$

Dimensionless groups

$Bo = D^* = \frac{D}{\sqrt{\frac{g\Delta\rho}{\sigma}}}$	Dimensionless vessel diameter also is the Bond number
$Fo = \frac{j_g^2}{g.h} = \frac{j_g^*}{h^*}$	Froude number
$h^* = h.\sqrt{\frac{g\Delta\rho}{\sigma}}$	Dimensionless height above the water surface
$j_g^* = j_g/\left(\frac{\sigma g\Delta\rho}{\rho_g^2}\right)^{1/4}$	Wallis number
$N_{\mu g} = \frac{\mu_g}{\sqrt{\sigma\rho_g\sqrt{\frac{\sigma}{g\Delta\rho}}}}$	Dimensionless viscosity
Ra	Rayleigh number
$We = \frac{j_g^2.D_H.\rho_l}{\sigma}$	Dimensionless viscosity

Greek symbols

μ_g	Gas viscosity$[N.s.m^{-2}]$
μ_l	Liquid viscosity$[N.s.m^{-2}]$
ρ_g	Gas density$[kg.m^{-3}]$
ρ_l	Liquid density$[kg.m^{-3}]$
$\Delta\rho = \rho_l - \rho_g$	Density difference$[kg.m^{-3}]$
σ	Surface tension$[N.m^{-1}]$
γ_i	Current correlation constants

determined by quantifying the amount of airborne aerosols. In the sector of water treatment, in order to separate solid from liquid phase, desalination plants use evaporator. The process is to entrain droplet by injecting steam. As the bubbles rise to reach the surface, they burst to generate small droplets that are partly entrained in the distillate (Cosandey, 1999). In horizontal and vertical separators in gathering centres, to separate phases (gas, oil and liquid), a mixture of gas–water-oil or gas-oil is feed into a static vessel. The inflow causes agitation of the interface by entraining gas into the mixture of oil-liquid in form of bubbles. This latter rise on the surface and burst producing droplets. Therefore, for phase separation, gas is exhausted by a vent at the top of the vessel, carrying liquid droplet with it. One of the principles of separation is coalescence. Coalescing is related to the agitation process. During coalescence, water droplets come together to form larger drops. In vane type mist eliminators, droplets are removed from the vapour stream through inertial impaction. The wet gas is forced to change direction causing mists droplets to strike the vanes and coalesce with other droplets eventually falling. However, some of the droplets escape without coalescing. Therefore, the amount of droplet needs to be quantified in order to measure the purity of the gas (Viles, 1993; Kharoua et al., 2013; Wurster et al., 2015).

In nuclear engineering, the Steam Generator Tube Rupture (SGTR) events may occur during an accident in Pressurized Water Reactor (PWR). The steam generator tube might experience degradations that cause leakage or rupture (Dehbi et al., 2016) (Fig. I-2, left). Water from the primary circuit passes in the secondary circuit by large quantities transporting fission products along. The steam generator is rapidly filled with water, and droplets might be released due to boiling from the pool to the environment through vents. Therefore, the quantification of these droplet is necessary from the design point of view.

In case of a severe accident in Boiling Water Reactor BWR, after the core damage, a mixture of steam/non-condensable gases and fission products (FPs) is transported via pipe into large pressure suppression pools (Fig. I-2, right). A fraction of the FPs while passing through a water pool will become trapped in the water pool and some of them will be re-entrained into gas atmosphere above water pool by the streaming gas due to the continuous heat release or boiling. The consequence of the gas release into the containment building atmosphere, also caused by release of H_2 and CO from MCCI, could jeopardize the containment integrity. Therefore, the building is depressurized using vents placed at a certain height above the water pool. The depressurization may induce boiling, and the rate of depressurization defines the hydrodynamic of the pool. High depressurization rates cause large agitation in water pool by producing large bubble (Kudo et al., 1994), whereas low depressurization rates produces small bubbles by agitates relatively smaller depth below the water surface (Freitag and Schmidt, 2017). In either case, the release of droplet from water pool as a function of the flow regime is inevitable. These droplets re-entrain contaminants (such as radioactivity carrying aerosol) and might contribute to their release to the environment in case of a containment breach or uncontrolled leakage.

The assessment of the entrainment phenomena is conducted by numerical simulation. Computational Fluid Dynamic (CFD) and Lumped

Parameter (LP) codes are used for this purpose. CFD simulations require computational resources to simulate small droplets in the micron range and provide as well results on the characteristics of the droplets including their size and velocity distributions at different height above the water pool, in addition to their concentration. Nonetheless, this amount of information is time consuming to acquire. Whilst LP codes are characterized by short time execution and providing results in a couple of minutes due to their empirical aspect. LP code are popular in simulating severe accidents scenarios in power plants.

Entrainment models found in literature have limited range of applicability in terms of the flow regime (high superficial gas velocity) and/or geometry. At the current knowledge, there is no model that englobes the full range of the boundary conditions (superficial gas velocity and geometry).

A prior understanding of the dynamics of the bubble is imperative, such as the effect of thermal hydraulics, physical properties of the liquid, bubble behavior at the surface of the pool before and after the burst for simple cases such as the study of a single bubble to quantify the entrainment. Then, the information on the single bubble could be translated to bubble swarm by analyzing the behavior of the bubbles at the water surface under low (Günther et al., 2003)and high gas flow rates. The main objective of this paper is to quantify the entrainment as a function of the hydrodynamics of the pool (flow regimes) for different scenarios that implies different geometries by one correlation.

2. Previous works

The droplets generated by a bubble break-up in the form of film or jet drops contribute to the entrainment taking into account the bubble size and flow regimes, hence interaction between bubbles.

Such droplets might be entrained by the streaming gas to different heights above the water pool. Kataoka and Ishii (Kataoka and Mamoru, 1983), subdivided these heights into three regions: 1) near the surface where the entrained droplets consist of all sizes, 2) the momentum controlled region which is considered as a transition region where droplets are either carried over or fall back, and 3) the deposition controlled region where droplets are small enough to be carried over and suspended, unless deposited onto wall. Fig. II-1 illustrate these three regions. Some authors conducted experiment to quantify the entrainment of droplet in the momentum controlled regions (Kim and No, 2003; Lebel et al., 2020; Garner et al., 1954), and others conducted experiment to measure the entrainment in the deposition controlled region (Freitag and Schmidt, 2017; Cosandey, 1999; Müller and von Rohr, 1997). The near surface region is a challenging zone to measure the entrainment due to high water surface agitation due to multiple bubble burst. However, since the entrainment consists of all droplet at the near surface region, Kataoka and Ishii (Kataoka and Mamoru, 1983), stated that the droplets mass flux is 4 times larger than the gas mass flux. This value is validated by previous authors as well (Bagul et al., 2019; Kim and No, 2003).

At low gas flow rates, the bubble range from spherical over elliptic to spherical cap (Clift et al., 1978). By reaching the surface, and due to hydrodynamics instabilities, the bubble disintegrates into droplets. This instability could be achieved by analysing the bond number through the critical bubble size.

Surface tension produces the centripetal force on the bubble lamellae sitting on the water surface. It is counteracted by the bubbles' internal overpressure. The bursting process is initiated by local thinning of the lamellae (which is more likely occur at the bubble foot) and hydrodynamic instability (Rayleigh–Taylor instability). Two families of drops are generated from the burst; film droplets produced from the bubble cap, and jet droplets, which are eventual consequence of film drops. The jet droplets are produced from the agitation of the water liquid inside the bubble after the burst, caused by the bubble pressure, and the drained film cap into the water bulk.

The mechanisms of droplet generation (c, d and e of Fig. I-1) are mostly encountered in pools. In a vessel filled with water, the bubbles are produced either by boiling due to continuous heat release or depressurization. The swell level of the pool surface depends on the gas injection patterns and pool dimensions.

Water droplets generated from the bursting bubbles at the water pool surface are ejected with different sizes and velocities in a parabolic

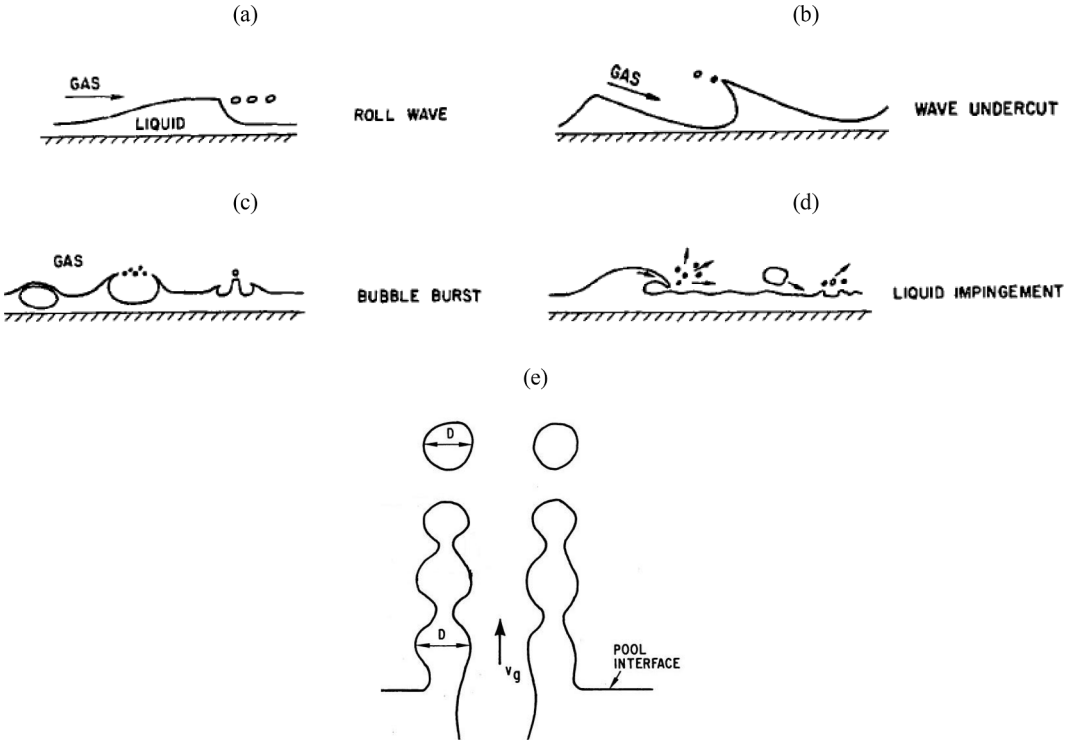

Fig. I-1. Droplets generation mechanisms (de Santiago and Marvillet, 1991; Kataoka and Mamoru, 1983).

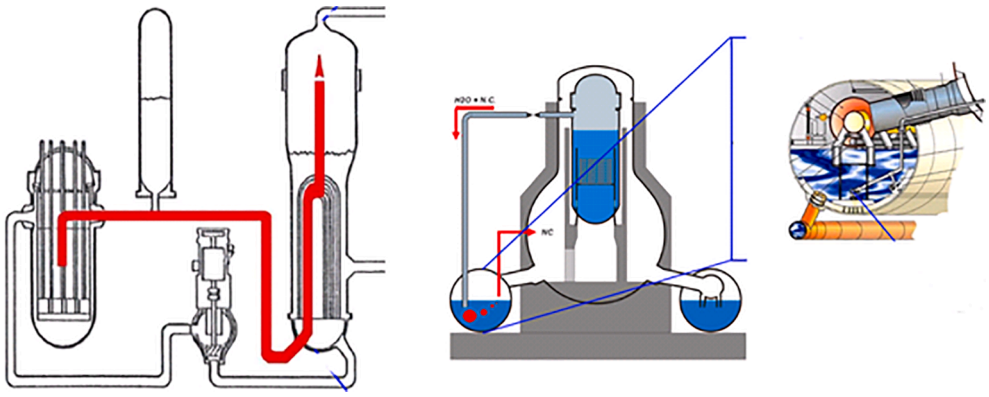

Fig. 1.2. Accident scenario in PWR (left), accident scenario in BWR (right) (Herranz, 2017).

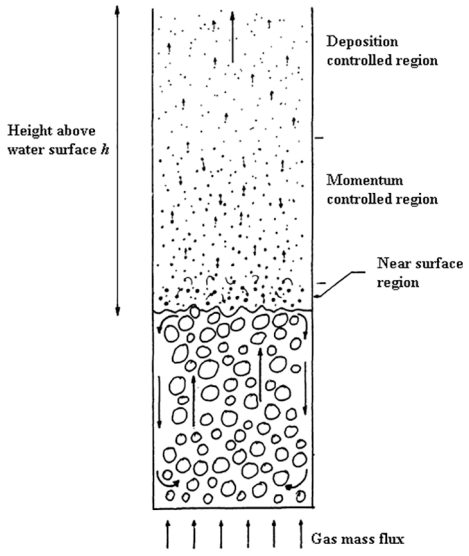

Fig. II-1. Entrainment of droplet at different regions above the water pool (adapted from (de Santiago, 1991)).

movement like a projectile. Spiel (1998a) and Spiel (1998b) investigated the angle of ejection of film droplets burst at the center, and found that the angles do not depend on the bubble size. Against the gas velocity, the droplets might settle down, or be carried over by the streaming gas to eventually stay airborne at specific heights. In Stokes flow regime, the terminal velocity, which is the maximum velocity reached by the droplet as it falls back in the vertical direction, of the droplets larger than the superficial gas velocity results in settling down. With terminal velocity smaller than the superficial gas velocity, the droplets continue to rise to the top vessel to stay volatile unless they deposit onto vessel structure or walls.

The entrainment showed a strong dependency on the superficial gas velocity and the height above the water surface (Kataoka and Mamoru, 1983) (Eq. (II-1)). At low superficial gas velocity, the entrainment consist of fine droplets. The fraction of these droplets and their size increase as the superficial gas velocity increase further. This could be summarized as shown in Table II-2:

The parameter in Table II-1 indicate the exponent of the superficial gas velocity for different flow regimes. The distance above the water pool has an opposite effect on entrainment comparing the superficial gas velocity. The entrainment is maximum near the surface and decreases as the distance above the pool surface increases due to turbulent diffusion.

There have been attempts to predict the entrainment theoretically by adopting statistical methods (Zenz and Weil, 1958; Andrews, 1960), however, some quantities such as droplets size and velocity distribution

Table II-2
Superficial gas velocity exponent with respect to zone above the water pool (Sterman et al., 1957).

Zone	I (near surface)	II (momentum controlled)	III (deposition)
n	$0 \rightarrow 1$	$3 \rightarrow 4$	$7 \rightarrow 20$
Condition for water droplet volatility	$v_t > j_g$	$v_t \leq j_g$	$v_t < j_g$

Table II-2
Summary of previous analytical works.

Authors	D_v (m)	D_p (m)	System	Pressure (bar)	Sup. gas velocity (m/s)
(Kruzhilin, 1951)	<0.3	<0.3	Steam – water Air – water	17 to 185	–
(Panasenko and Antonov, 1959)	0.238	0.238	Steam – water Air – water	17 to 185	0.075 to 0.56
(Sterman, 1958)	0.238	0.238	Steam – water Air – water	17 to 185	0.27 to 0.56
(Rozen et al., 1970)	<0.3	<0.3	Steam – water Air – water	–	–
(Kataoka and Mamoru, 1983)	<0.3	<0.3	Steam – water Air – water	1 to 185	0.5 to 2.0
(Cosandey, 1999)	1.5	0.6	Steam – water Air – water	2 to 6	0 to 0.0044
(Dapper, 2009)	3.2	1.4	Steam – water Air – water	2	0 to 0.05

was unavailable at that period of time. Even though, such quantities are extremely difficult to measure due to the size of droplet and their interactions.

Nevertheless, there are a fair amount of empirical correlation to predict the entrainment (Kruzhilin, 1951; Sterman et al., 1958; Golub, 1970; Panasenko and Antonov, 1959; Reeks et al., 1988).

Kruzhilin (1951)) adopted a semi-empirical method to determine the entrainment, assuming that the contribution of the film droplets

produced by the disintegration of the bubble cap is neglected. The droplets that contribute to the entrainment are those carried away by sufficient gas kinetic energy, and interaction between droplets is neglected. The amount of entrained droplets depends upon the kinetic energy of the gas and physical properties of the liquid. Based on a dimensional analysis, Kruzhilin (Kruzhilin, 1951) obtained the following:

$$E_{fg} = C_K \frac{\rho_g j_g^4}{\sigma g}\sqrt{\frac{\rho_g}{\rho_l}} \tag{I.2}$$

C_K is determined experimentally.

The effect of height is not considered in the formulation of Kruzhilin (1951), thus, his model is suitable to calculate the entrainment near the water surface. The correlation of Kruzhilin is limited, for the reason that the entrainment depends only of jet drops. Moreover, the superficial gas velocity in Eq. (II-2) is power 4, which means at such superficial gas velocity, the only droplet that can be generated are from the liquid ligaments. Thus, neglecting the film droplets in Kruzhilin's assumptions is consistent with Eq. (II-2). Moreover, the omission of the droplets interaction might also have a noticeable impact on entrainment, since the outcome of such interactions might be coalescence or breakup. The void fraction increase with increasing gas velocity, therefore formation of large bubbles.

Panasenko and Antonov (Panasenko and Antonov, 1959), later on, decided that the formulation of Kruzhilin (Kruzhilin, 1951) needed to be evaluated and adapt it to their considerations. This implies introducing the height of the vapour space above the water surface.

$$E_{fg} = 1.96{*}10^7 \frac{(\rho_g g)^{0.48}\mu_l^{1.8} j_g^{1.96}}{g^{0.08}(\rho_l g)^{1.03}\sigma^{1.25}h^{1.18}} \tag{I.3}$$

Eq. (II-3) was correlated with experimental data of Sterman et al. (1957), Sterman et al. (1958) and Styrikovich et al. (1955).

Sterman (1958) studied the effect of pressure on pool entrainment based on dimensional analysis in churn turbulent flow regime for pressure up to 185 bar. The Eq. (II-4) is based on previous experiments (Sterman et al., 1957; Styrikovich et al., 1955; Sterman et al., 1958; Sterman, 1952; Kolokoltzev, 1952).

$$E_{fg} = 6,1.10^9 \frac{\left(\frac{j_g^2}{gh}\right)^{1.38}\left(\frac{a}{h}\right)^{0.92}}{\left(\frac{ga^3}{\nu_l^2}\right)^{1.1}\left(\frac{\Delta\rho}{\rho_g}\right)^{1.124}} \tag{II.3}$$

$$a = \left(\frac{\sigma}{g\Delta\rho}\right)^{0.5} \tag{II.4}$$

The parameter h in Eqs. (II-3) and (II-4) is the height above the water surface. This height decreases with increasing gas flow rate.

Rozen et al. (1970) considered a normal law to describe the droplet size distribution, and analyse the entrainment from the forces acting on a single droplet; weight, buoyancy and drag. Then, he validated the model against experimental data to find the following relationship (Eq. (II-5)):

$$E_{fg} = \left[A.K^{0,5} + B.K^{2,1}\right]\sqrt{\frac{\Delta\rho}{\rho_g}}e^{-0,23h/D_H} \tag{II.5}$$

With

$$A = 9,011.10^{-5}\Delta\rho^{0,625}\rho_g^{-0.25}\sigma^{-0,375}g^{-0,25}$$
$$B = 0,753\Delta\rho^{1,025}\rho_g^{-0.5}\sigma^{-1,575}g^{-1,25}$$
$$K = d_{dr}j_g$$

From this equation, one might deduce that the entrainment is decreasing with increasing height above the water pool.

Kataoka and Mamoru (1983) developed a set of correlations that includes three equations corresponding to three zones above the water pool, as shown in Table II-1.

The first zone and the second zone are controlled by the momentum of the droplets, and the third zone is controlled by the deposition.

These zones are determined by analysing the main parameters having notable effect on entrainment: superficial gas velocity and height above the water pool. Kataoka and Mamoru (1983) considerations on quantifying the entrainment are different from previous work (Sterman, 1958; Panasenko and Antonov, 1959; Styrikovich et al., 1955; Kruzhilin, 1951)). Assuming that the droplets travel in a vertical direction – from zone I to zone III – gives rise to another parameter affecting the entrainment, which is the height above the water surface. This parameter appear in previous correlation, however it has not been addressed explicitly. The height itself depends on the composition of the atmosphere and pool's thermal hydraulics (Cosandey, 1999).

The Kataoka and Ishii's (Kataoka and Mamoru, 1983) correlations for different regions above the water pool from the surface to the uppermost part of the vessel are:

$$For\ the\ near\ surface\ region\ E_{fg}(h,j_g) = 4,84.10^{-3}\left(\frac{\rho_g}{\Delta\rho}\right)^{-1,0} \tag{II-6}$$

Momentum controlled region

$$E_{fg}(h,j_g) = 2,213N_{\mu g}^{1.5}D_H^{1,25}j_g^{*}h^{*-1}\left(\frac{\rho_g}{\Delta\rho}\right)^{-0,31} \tag{II-7}$$

$$E_{fg}(h,j_g) = 5,417.10^6 j_g^{*3}h^{*-3}N_{\mu g}^{1.5}D_H^{1,25}\left(\frac{\rho_g}{\Delta\rho}\right)^{-0,31} \tag{II-8}$$

$$E_{fg}(h,j_g) \propto \left(\frac{j_g^*}{h^*}\right)^{7\ 20} \tag{II-9}$$

$$E_{fg}(h,j_g) = 7,13.10^{-4}j_g^{*3}N_{\mu g}^{0.5}\left(\frac{\rho_g}{\Delta\rho}\right)^{-1,0}e^{-0,205\left(\frac{h}{D_H}\right)} \tag{I-10}$$

Eqs. (II-6) through (II-10) was validated against data of Styrikovich et al. (1964), Garner et al. (1954), Sterman et al. (1957); Sterman (1958), Styrikovich et al. (1964)), Golub (1970) and Rozen et al. (1976a).

The range of validity of the Kataoka and Mamoru (1983) for superficial gas velocity is $j_g \in$ [0.5–2] m/s, which correspond to churn turbulent flow regime.

Cosandey (1999) and Cosandey and Von Rohr (2001) developed a correlation to quantify the re-entrained soluble and insoluble particle from droplets entrainment under very low gas flow rates as a consequence of vessel slow depressurization from 6 bar to 2 bar, using data from his own experiments. The correlation is based on the dimensional Buckingham theory, which leads to a group of dimensionless numbers.

$$E_{fg} = k_1.x_{BP}^{k_2}We_{cont}^{k_3}Fr_{cont}^{k_4}(1+Ra)^{k_5} \tag{I-11}$$

The parameters $k_i$in Eq. (II-11) are determined experimentally.

Dapper (2009) developed a correlation to quantify the re-entrainment of aerosol in a boiling pool in the deposition controlled region. The correlation depends on the superficial gas velocity and the bubbling pool cross section.

$$r = \frac{\dot{V}_{dr}\rho_{pool}}{M_{pool}} \tag{I-12}$$

With the suspended droplet volume flow rate

$$\dot{V}_{dr} = A.j.e^{f.d_{dr}} \tag{I-13}$$

$$d_{dr} = \frac{a'}{j_g^{b'}}\sqrt{\left(\frac{\mu_g}{\rho_l}\right)} \tag{I-14}$$

The table below summaries the previous developed correlations.

The previous correlations are limited to a specific geometry and flow regime. Correlation developed by Dapper (2009) and Cosandey (1999) have been conducted in large vessel (simulation of BWR containment building during late phase of a severe accident) in low gas flow rates (bubbly flow regime). While (Kruzhilin, 1951; Panasenko and Antonov, 1959; Sterman, 1958; Rozen et al., 1970; Kataoka and Mamoru, 1983) have been developed for smaller vessel and under high gas flow rates. At the current knowledge, there has not been found a correlation that covers the full range of superficial gas velocity and applicable for several geometries for containment applications taking into account the thermal–hydraulic conditions.

3. Correlation for entrainment amount

In water pool of diameter large than approximately 0.2 m, two flow regimes could be defined as a function of superficial gas velocity; bubbly flow regime and churn turbulent flow regime. Two flow regime could be identified which are attributed to bubble flow regime; homogeneous flow regime and inhomogeneous flow regime (Shah et al., 1982; Ruzicka et al., 2001). In homogeneous flow regime, the bubble could be assume uniform in size, while in inhomogeneous regime the bubble follow a size distribution (typically lognormal (Berzal et al., 1996)). Some authors refer to inhomogeneous flow regime as the transition regime (Freitag and Schmidt, 2017), since it follows the homogeneous flow regime (also referred as bubbly flow regime) to churn turbulent flow regime. This terminology is adopted in this paper henceforth.

In this section, an empirical correlation to predict the entrainment amount using data from the open literature for bubbly flow, transition and churn turbulent flow regimes.

3.1. Bubbly flow regime

This flow regime is characterized by the formation of quasi-uniform bubbles of typical size of 2 mm in the water pool. As they rise toward the surface, coalescence might occur between bubbles to form bigger one (Fig. III-1). Bubble coalescence is not a common phenomenon in bubbly flow regime at the surface, however it might occur occasionally.

The gas velocity to create such bubbles is 0.05 m/s (Shah et al., 1982).

The experiments of THAI (Schmidt et al., 2015; Freitag and Schmidt, 2017; Cosandey, 1999), and REVENT (Müller and von Rohr, 1997) provide data for this range of superficial gas velocity. As shown in the figure below, the entrainment increases slightly with an exponential fit to reach a maximum value of 1.2E-04 which corresponds to a ratio j^*/h^* = 3.4E-6.

The correlation for this flow regime has the following form:

$$E_{fg} = \gamma_1 . exp(\gamma_2 . \frac{j^*}{h^*}) \quad \text{(III-1)}$$

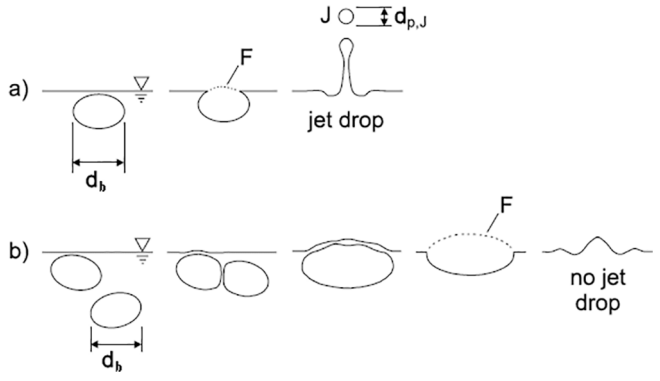

Fig. III-3. Difference in the breakup mechanism for a single (a) and multiple (b) bubbles due to coalescence (figure adapted from (Günther et al., 2003)).

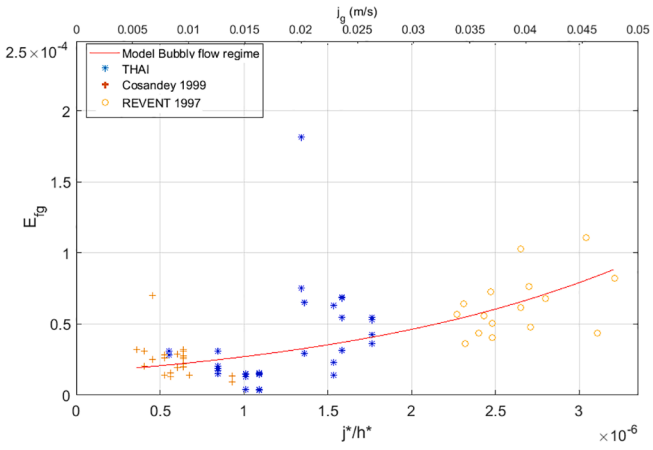

Fig. III-3. Entrainment correlation for Bubbly flow regime.

For superficial gas velocity values<0.05 *m/s*, corresponding to j*/h*=3.4E-6 and a height from $h = 3$ m to $h = 8$ m above the water surface, the coefficients of Eq. (III-1) (Table III-1) are calculated via nonlinear regression analysis, with the goodness of fit of $R^2 = 0.525$. The scatter of data has an impact on the R^2 value, with a value 1 denoting a perfect fit without scatter:

The entrainment in the THAI facility was measured at $h = 8$ m, while Cosandey (1999) measured the entrainment at $h = 3$ m. At such heights, the entrainment corresponds to the entrainment in the "deposition region" (Kataoka and Mamoru, 1983).

3.2. Transition regime

This flow regime takes place in the transition range between bubbly flow and churn turbulent flow regime. It is also referred as the heterogeneous flow regime due to the formation of bubble of different sizes. Such bubbles can reach a size of 5 mm in the water pool, and when reaching the surface, larger bubble might be formed due to coalescence (Shah et al., 1982; Ruzicka et al., 2001). Coalescence might also occur inside the pool.

The data used to develop the correlation is from REST (Bunz et al., 1992) and THAI (Freitag and Schmidt, 2017; Schmidt et al., 2015).

The entrainment decreases smoothly from 1.4e to 4 (j^*/h^*=3.4E-6) to a minimum value of 2.5e-5 (j^*/h^*=1.9E-5) which corresponds to superficial gas velocity of 0.1 m/s (Fig. III-3).

The correlation for this flow regime is described by a linear function with a negative slope:

$$E_{fg} = \gamma_3 . \frac{j^*}{h^*} + \gamma_4 \quad \text{(III-2)}$$

For superficial gas velocity $0.05\ m/s < j_g < 0.1\ m/s$ corresponding to a ratio 3.4E-6 < j^*/h^*< 1.9E-5, the coefficients of Eq. (III-2) are calculated with the goodness of fit of $R^2 = 0.570$ (Table III-2):

Based on test data of WH-24 and literature findings (Bunt et al., 2015), a noticeable uncertainty should be considered with respect to the entrainment rate value at given superficial velocity. In THAI experiments, this uncertainty was a factor of 2 to 5.

Table III-1
Correlation constants for bubbly flow regime.

condition	γ_1	γ_2
$j \leq 0.05$ m/s $j^*/h^* \leq 3.4e{-}6$	1.576e-5	5.353e + 5

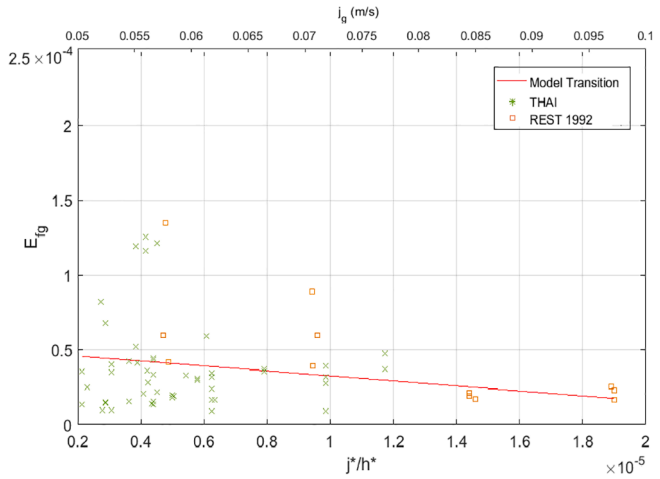

Fig. III-3. Entrainment correlation for Transition regime.

Table III-2
Correlation constants for Transition regime.

condition	γ_3	γ_4
0.05 m/s $< j_g \leq$ 0.08 m/s 3.3e-6 $< j^*/h^* \leq$ 1.9e-5	−6.666E−6	4.019E−5

3.3. Churn turbulent flow regime

For superficial gas velocity value above 0.1 *m/s*, the flow regime is attributed to churn turbulent

Unsteady flow pattern with channelling occurs in the water pool and the main characteristics of this regime is the formation of large pockets of gas accompanied by small bubbles. Also, this flow regime is marked by the extreme high agitation of the surface of the pool (Shah et al., 1982; Ruzicka et al., 2001).

The data supporting this flow regime was obtained from the open literature, and are up to date (Lebel et al., 2020; Kim and No, 2005; Zhang et al., 2016; Garner et al., 1954; Golub, 1970).

In Fig. III-4, as the entrainment ranges from 4E to 5 to approximately 10, a double logarithmic scale has to be used to cover the complete range in this flow regime. As shown in the figure, the entrainment increases sharply as a function of the ratio j^*/h^*, and the correlation follows the trend of the data. The correlation is described by a nonlinear function and has the following form:

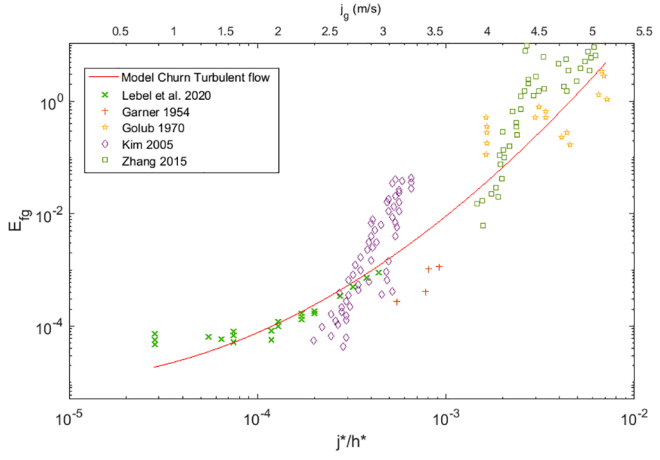

Fig. III-4. Entrainment correlation for Churn Turbulent flow regime.

$$E_{fg} = \gamma_5 * \left(\frac{j^*}{h^*}\right)^{\gamma_6} \quad \text{(III-3)}$$

For superficial gas velocity above 0.1 *m/s* corresponding to a ratio j^*/h^*=2E-5, the coefficients of Eq. (III-3) are calculated with the goodness of fit of $R^2 = 0.874$ (Table III-3):

In Fig. III-5 the predicted and measured entrainments are compared for the complete range of regimes. As it shows, there is a fair agreement between the predictions and the experimental data (Lebel et al., 2020; Kim and No, 2005; Zhang et al., 2016; Garner et al., 1954; Golub, 1970; Bunz et al., 1992; Freitag and Schmidt, 2017; Müller and von Rohr, 1997; Cosandey, 1999). The scatter on both sides of the y = x line can be explained by the large standard deviation of the entrainment from experimental data.

In conclusion, the empirical correlations obtained by Eq. (III-1) through (III-3) allows the prediction of entrainment for bubbly flow regime, the transition regime and churn turbulent flow regime for heights above the water pool up to 8 m (Freitag and Schmidt, 2017).

In the next section, a discussion follows in support of the current empirical correlation by analyzing the dynamics of the bubbles, and the ability of such bubbles to produce droplets.

4. Discussion

In this section, the present empirical correlation is discussed as a function of the trends against experimental data. Large amount of data to validate the model are available as mentioned in the previous section on entrainment of droplets for bubbly flow, transition and churn turbulent flow regime.

In this work, in order to calculate the entrainment and compare different results from previous data set, it was found that the ratio of the dimensionless superficial gas velocity to the dimensionless height above the water pool is the adequate independent variable that can be used to take into account the flow regime and the geometry effect. The ratio j_g^*/h^* could be attributed to the Froude number *Fr,* by doing the following approximation$\Delta\rho \approx \rho_l$. For extremely high pressure, this approximation cannot be held, since the fluid density increase and the gas density increasing as the pressure increases.

The main objective of this section is to show the order of magnitude of different results and to support the current model by physical facts.

4.1. Bubbly flow regime

Fig. III-2 shows the entrainment correlation using data of THAI, Cosandey, and REVENT experiments for bubbly flow regime. The entrainment varies between a minimum value of 1E−6 and a maximum value of 1.2E−4. The range of gas velocity used by Cosandey is from 0.0008 m/s to 0.0044 m/s, whereas THAI covered the full range of gas velocity for bubbly flow regime (from 0 to 0.05 m/s). The Cosandey's experiments (Cosandey, 1999) were conducted under slow depressurization conditions from 6 bar to 2 bar. The bubble size measured in such conditions was about 2 mm. Similarly, the bubble size was about 2 mm in the REVENT experiments where a small range of superficial gas velocity from 0.009 m/s to 0.01 m/s was imposed. The characteristics of such flow regime is that the bubbles in the water pool could be assumed to be uniformly sized (Shah et al., 1982). When reaching the surface, these bubbles produce two families of droplets which eventually could be entrained by the gas coming out: film droplets coming from the cap,

Table III-3
Correlation constants for Churn Turbulent flow regime.

Condition	γ_5	γ_6
0.1 m/s $< j_g$ 2E-5 $< j^*/h^*$	1.22e + 7	4.748–7.838

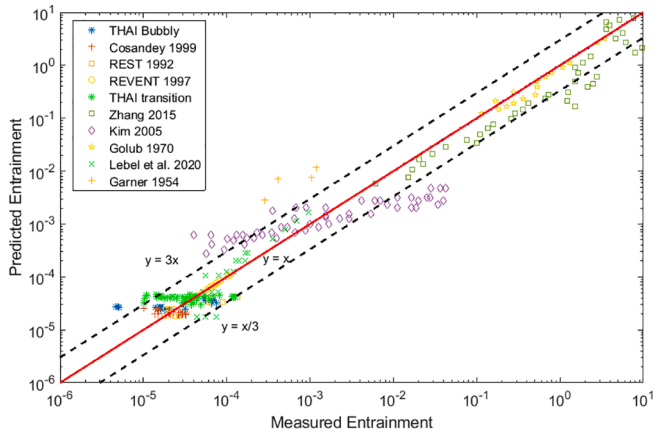

Fig. III-5. Comparison of the calculated (current correlation) and measured entrainment ((Lebel et al., 2020; Kim and No, 2005; Zhang et al., 2016; Garner et al., 1954; Golub, 1970; Bunz et al., 1992; Müller and von Rohr, 1997; Cosandey, 1999)).

and jet drops coming from the crater formed after the bubble burst (Spiel, 1998a; Spiel, 1998b). The film droplets size (order of 10 μm) is much smaller than the jet drops (order of 100 μm). These two families of droplets contributes noticeably to the entrainment (Garner et al., 1954; Spiel, 1998a; Spiel, 1998b; Blanchard and Syzdek, 1988).

For an air–water system, the bubble size increase with increasing gas velocity as investigated by (Jamialahmadi and Muller-Steinhagen, 1990) as shown in Fig. IV-1. The bubble size is constant for superficial gas velocity up to approximately 4 cm/s, and then the bubble size increases as the superficial gas velocity increases further. Expect the correlation of Akita and Yoshida (Akita and Yoshida, 1974), it contradicts the this trend (Fig. IV-1). The reason given by (Jamialahmadi and Muller-Steinhagen, 1990), is that the correlation of Akita and Yoshida is limited to single orifice spargers (Shah et al., 1982).

Fig. IV-1 allows providing a link between superficial gas velocity and bubble size at surface However, It is necessary to know at what extent this bubbles size – superficial gas velocity dependence should be applied. Therefore, the effect of thermal-hydraulics, and physical properties of the gas-fluid should be taking into account.

The pressure in the experiments used to develop the current correlation for bubbly flow regime is from 2 bar to 6 bar. At this range of pressure, the bubble size distribution is affected slightly compared to bubbles submitted to very high pressure (Cosandey, 1999). Cosandey (1999) noticed a decrease in entrainment measurement by a factor of 2 when decreasing the pressure from 6 bar to 2 bar, however this decrease is in the range of uncertainty. Nevertheless, the effect of pressure on bubbly size distribution is substantial at very high pressures as discussed earlier (Lin et al., 1998). In bubbly flow regime ($j_g < 0.05$ m/s), at pressure up to 6 bar (Cosandey, 1999), bubbles have the ability to produce film and jet droplets. The production of film droplets is at its peak (Blanchard and Syzdek, 1988), however, fewer jet droplet are produced comparing to smaller bubble size (Koch et al., 2000).

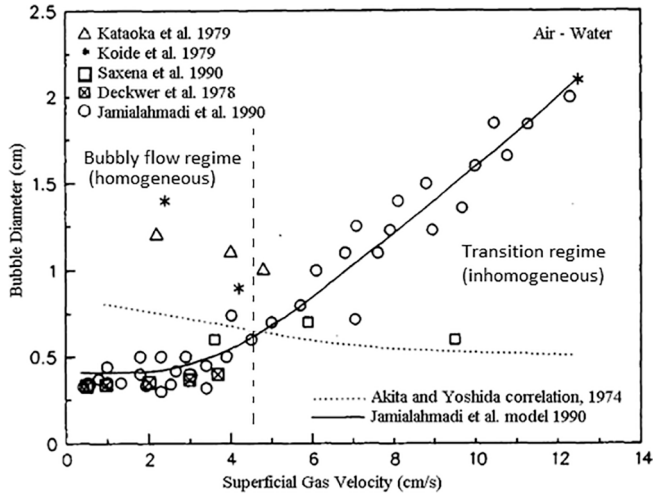

Fig. IV-1. Average bubble size as a function of Superficial gas velocity, adapted from (Jamialahmadi and Muller-Steinhagen, 1990).

The production of droplet from film cap and the jet were also investigated by Günther et al. (2003) for low superficial gas velocity similar to bubble flow condition of (Cosandey, 1999) producing bubble of around 2.98 mm diameter, from a sparger in a 100 mm diameter pool. The investigation mainly conducted by Günther et al. (2003) aimed to compare the droplets production from single bubble against multiple bubbles (bubbly flow regime). The main outcome of their experiments was that the number of droplets (jet and film) produced by multiple bubbles was less than the number produced by a single rising bubble (discrete bubbles one after another).

As it shows in Fig. IV-2, the probability of multiple bubbles case to produce droplet is less than the probability for single bubble case. Bubbles tend to merge at the surface of the pool to form large ones (Günther et al., 2003). Eventually bigger bubbles produces limited number of droplet, and sometime having the tendency to not produce them (Koch et al., 2000). Spiel (1998a) and Spiel (1998b) stated that the film opening speed S_f, caused by the bubble burst, decrease with increasing bubble size as $S_f = 27.\exp(-d_b/7.862)$, and that the film thickness increase with decreasing the film opening speed (film thickness could be calculated by Taylor-Culick velocity $S_f = V_{tc} = \sqrt{2\sigma/\rho h_{film}}$). Then, if one considers the film Weber number, $We_{film} = \frac{\rho S_f^2 l_{film}}{\sigma}$ with l_{film} being the film length, and according to Spiel (1998a) and Spiel (1998b), as the bubble size increases, the film velocity decreases and the We_{film} decreases too. The surface tension will become substantial and the film will find difficulties to break up, therefore the number of the film droplets decreases.

4.2. Transition regime

Fig. III-3 presents experiments supporting the transition regime to predict the entrainment. In the experiment of REST (Bunz et al., 1992) the range of superficial gas velocity was from 0.05 m/s corresponding to an entrainment of 1.4E-4 to a superficial gas velocity of 0.08 m/s corresponding to an entrainment of 3E-5. In the THAI experiments, , for superficial gas velocities ranging from 0.025 m/s to 0.13 m/s, entrainment values between 3E and 6 to 3E-4 are obtained whereas the entrainment reduces towards larger superficial velocities (Schmidt et al., 2015). Under such range of superficial gas velocities, the bubble cannot be considered uniformly sized (Shah et al., 1982). Large bubbles up to 1 cm are formed in the water pool with tendency of coalescence to occur (Ruzicka et al., 2001) inside the pool and at the surface to eventually form even larger bubbles. Consequently, the presence of these large bubbles at the surface tends to reduce the entrainment (Cosandey, 1999).

The arguments given for the bubbly flow regime is applicable for the transition regime, since the bubble is well defined in shape and size.

In the experiments of THAI (Freitag and Schmidt, 2017) and REST (Bunz et al., 1992), the pressure imposed was from 1 bar to 2.5 bar and superficial gas velocity from 0.05 m/s to 0.1 m/s.

The size of the bubbles in the transition regime, tend to produce only film droplets (Zhang et al., 2012; Koch et al., 2000). As for jet droplets, bubbles of diameter larger than 5 mm, practically do not produce jet droplets (Koch et al., 2000), since bubbles of this size contain low energy comparing to smaller ones (Cosandey, 1999).

As for the droplet produced by the film, their number are reduced

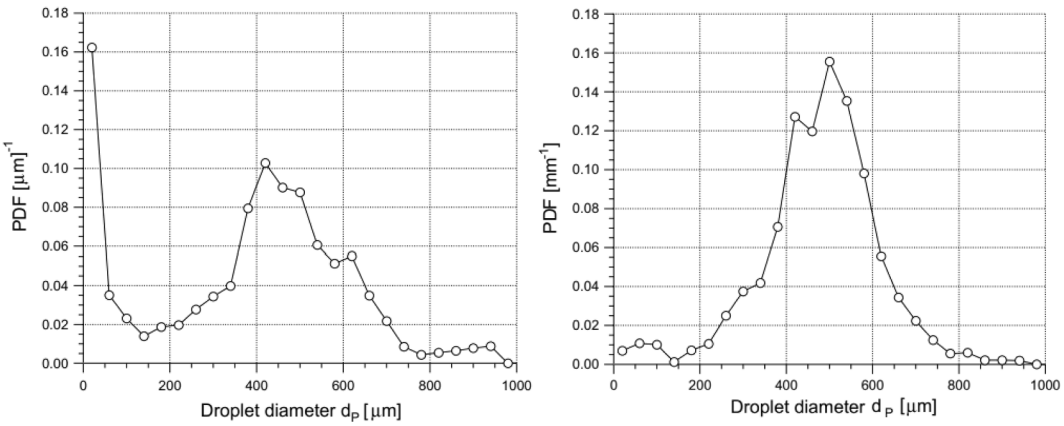

Fig. IV-2. Probability density function PDF for droplet diameter for (left) multiple bubble and (right) single bubble (Günther et al., 2003).

with increasing bubble size after a typical size of 2.5 mm as investigated by (Blanchard and Syzdek, 1988; Spiel, 1998a; Spiel, 1998b; Resch and Afeti, 1992).

Moreover, (Lhuissier and Villermaux, 2012) demonstrated experimentally that the maximum bubble size from which the number of film droplets begins to decrease could be calculated by R_0 3.8a which gives a value of around 10 mm.

Additionally, the reason behind this lack of film droplet production might also be related to the drainage of film cap at the surface. In general, bubbles burst occur due film thinning, but the burst occurs as well due to instabilities. Large bubbles loses their stability before the complete film drainage, eventually, very few droplet will be produced (Lhuissier and Villermaux, 2012).

The capillary length, which is the maximum stable bubble size, could be calculated as a function of pressure as shown in Table IV-1. The capillary length decreases as the pressure increase as explained earlier on the effect of pressure on bubble size. In bubbly flow regime, the bubble size compete against the capillary length, thus, sometimes they will have enough time to drain the film cap and entrain more droplets, and sometimes they burst immediately due to bubble instabilities by the formation of large bubbles because of coalescence as mentioned earlier. In the transition regime, and as the bubble swarm reach the surface, the tendency to form larger bubbles than the capillary length is elevated, therefore, they lose their stability and burst quite immediately. In addition, these large bubbles will not have the required time to drain the film cap, resulting in entraining very few droplets.

The impurities might affect as well the film droplets production to a very small amount. A recent work published by Wei et al. (2020) demonstrated that the production of film droplet by large bubbles could be reduced in the presence of insoluble aerosols due to agglomeration. This latter showed to be relevant when increasing water temperature. The bubble is able to produce droplets before aerosol agglomeration at the surface, and the agglomeration occurs with increasing temperature (Wei et al., 2020).

In transition regime, the main characteristic is the formation of large bubbles inside the pool and at the surface by coalescence. Such bubbles are extremely instable as they grow in size, and tend to produce less droplet, thus, less entrainment. However, the situation changes when the gas velocity increase further in churn turbulent flow regime, where the information about bubble size is lost.

Table IV-1
Capillary length as a function of pressure.

Pressure (bar)	2	4	6
Capillary length (mm)	2.5	2.35	2.24

4.3. *Churn turbulent flow regime*

Superficial gas velocity superior to 0.1 m/s characterizes this flow regime. Lebel et al. (2020) used high superficial gas velocity from 0.1 m/s, which corresponds to a minimum entrainment of 1E-4 to a superficial gas velocity of 0.4 m/s with a maximum entrainment of 1E−3. Garner et al. (1954) obtained entrainment values from 4E to 5 to 1E-3 corresponding to superficial gas velocity of 0.46 m/s to 1.4 m/s. Kim and No (2005) measured an entrainment value of 5E-2 for superficial gas velocity of 0.35 m/s, Zhang et al. (2016) recorded a minimum entrainment of 6E-3 for $j_g = 0.98$ m/s to a maximum value of 4 for $j_g = 5.41$ m/s. The values obtained by Rozen et al. (1976b) lies between the values obtained by Zhang (Table IV-2 shows a comparison between experimental data). An exponential increase of entrainment is indicated as a function of superficial gas velocity. In this flow regime, the main characteristic is the creation of large irregular pockets of gas surrounded by small bubbles in the water pool. The droplets production mechanism is excessively different from the bubbly flow regime and the transition regime. The increase of superficial gas velocity in such flow regime has two consequences, both of which enhance entrainment: on the one hand, increasing superficial gas velocity creates more ligaments of water at the surface, implying the generation of large droplets. On the other hand, increased velocity offers the possibility to lift these larger droplets (Kataoka and Mamoru, 1983; Cosandey, 1999). Eventually the regenerated droplets contribute substantially more to the entrainment than in bubbly flow and transition regimes (See Table IV-3).

The effect of pressure on this flow regime as mentioned earlier is substantial especially at very high pressure. The paper of Sterman et al. (1957) could not be found to analyze effect of thermal–hydraulic in churn turbulent flow regime. Sterman used gas velocity up to 1.2 m/s and pressure up to 185 bar for a water steam system (appendix section of (Yeh and Zuber, 1960)). The entrainment decreases as the pressure increase in the experiment of (Sterman et al., 1957), from an entrainment of 2e−2 corresponding to a 1 bar, to 4e-4 corresponding to a pressure of 185 bar. This is a decrease by 2 order of magnitude, and the reason could be related the decrease in bubble to a much smaller size which

Table IV-2
Correlation's aspect and uncertainty.

Authors	Analytical	Empirical	Uncertainty
Current Correlation	No	Yes	2E-5 – 5E-5 For bubbly and transition flow regime
Sterman (Sterman, 1958)	Yes	Yes	Not available
Panasenko (Panasenko and Antonov, 1959)	Yes	Yes	Not available
Kataoka (Kataoka and Mamoru, 1983)	Yes	Yes	Not available

Table IV-3
Comparison of set ups of entrainment experiments.

Authors	H (m)	D_H(m)	h (m)	D_p (m)	P (bar)	j_g (m/s)	E_{fg}
THAI Freitag and Schmidt, 2017; Schmidt et al, 2015	9	3.2 or 1.6	5.9 to 8.2	1.4 or 1.6	2.5	0 to 0.1	8e-5–1.2e-4
Cosandey (Cosandey, 1999)	3	1.5	2	0.6	2 to 6	0 to 0.0044	2.5e-5–8e-5
ALPHA (Kudo et al., 1994)	5.7	3.9	1.2	0.305	1 to 15	0.04	7e-5
REVENT (Müller and von Rohr, 1997)	3	1.5	2	0.6 to 1.5	4	0.01	6.5e-5–1.3e-4
REST (Bunz et al., 1992)	1.5	1.5	0.14	0.108	1	0.08	1.3e-4–2e-5
(Lebel et al., 2020)	1.49	0.19	0.6	0.19	1	0.37	9e-4–1e-3
(Zhang et al., 2016)	2.2	0.38	0.187 to 1.53	0.38	1	0.98 to 5.41	6e-3–10
(Kim and No, 2005)	2	0.3	1.9	0.3	1	0.35	4e-5–5e-2
(Garner et al., 1954)	1.37	0.3	0.61	0.61	1	1.2	2e-4–1.1e-3
(Golub, 1970)	0.1 to 2.2	0.2	–	0.2	1	0.5 to 2	1e-1-3

eventually entrained less droplets relatively to churn turbulent flow regime.

In the experiment of (Zhang et al., 2016), the surface of the pool at the simulated superficial gas velocity up to 5 m/s, illustrate the enhancement of entrainment in this flow regime.

It can be seen that at such gas flow rates, the two-phase flow mixture is very agitated and could be assimilated to a jet/fountain type flow, which makes difficult to differentiate the overflow from entrainment.

In this flow regime, droplets are generated only by detachment. The liquid ligaments lose the stability due the high gas momentum exchange, which lead to the creation of droplet of multiple sizes quickly. Surface tension forces cease to be important, thus even with the presence of impurities in the liquid pool, it does not affect the droplet formation process nor their stability for Newtonian liquid (Clift et al., 1978).

The weber number We, which is the suitable quantity to study the liquid sheets dynamic stability, depends on the square of superficial gas velocity. Thus, as the superficial gas velocity increase rapidly, the Weber number increases exponentially. In such case, the surface tension has practically very weak effect, and the dominant term is the inertial term. Therefore, the liquid ligaments detached very fast as a results of momentum exchange and the formation of droplets increase with superficial gas velocity.

In churn turbulent flow regime, the overflow at the surface at some extent is referred by some authors as “droplet flow regime” (Colomer and Rogers, 2006), since all what could be seen are droplet detaching from the ligament due to high gas flux. This condition could be assimilated to a fluidized bed of droplet in the continuum phase (gas) (Colomer and Rogers, 2006). In terms of aerosol release from water pool, these droplets are easy to retain, as they are large enough to capture. Oppositely, droplets generated in bubbly flow regime are so tiny, which make them hard to retain (Dehbi et al., 2016).

The general trend as shown in Fig. IV-3 is that the entrainment increases as the gas velocity increases, and decrease as the distance from the water surface increases. This decrease is due to the diffusive transport. For steady state conditions, with a given superficial gas velocity, and considering the component above the pool surface, h, the entrainment decreases exponentially as the h increases.

Fig. IV-3 represent the current correlation compared to previous semi-empirical correlation of Sterman (1958), Panasenko and Antonov (1959) and Kataoka and Mamoru, (1983). Sterman and Panasenko and Antonov correlations underpredits the entrainment, while Kataoka and Ishii correlation over predicted the entrainment in the churn turbulent flow regime with respect to the current correlation. This might be related to the boundary condition of experimental data used by the previous authors to develop their correlations such as pressure which has showed to have a great influence on bubble dynamics and bubble geometry (Lin et al., 1998; Wilkinson and Laurent, 1990). The correlations of Sterman (1958), Panasenko and Antonov (1959) were developed under pressures up to 185 bar. At such pressures the bubble column is affected noticeably (Lin et al., 1998), reduce the bubble size until it become stiff and does not breakup anymore. Lin et al. (1998) measured this bubble size experimentally and is 0.5 mm diameter. These bubble class showed to produced large amount of jet droplets (Koch et al., 2000), and practically no film droplets (Lhuissier and Villermaux, 2012). Analytically, and assuming no droplets nor bubble interactions, the entrainment of such droplet increase with increasing superficial gas velocity (under pressure of 185 bar). Experimentally, these interactions are inevitable, and the droplet production is a function of the bubble size. Thus, the entrainment predicted by Sterman (1958), Panasenko and Antonov (1959) have smaller slope and necessitate more superficial gas velocity to entrain droplets. Whereas under different conditions (pressure up to 16 bar), the present correlation under the same range of superficial gas velocity attributed to churn turbulent flow regime, the entrainment increase exponentially due to rapid momentum exchange between gas and water ligament. Under churn turbulent flow regime, it only need smaller superficial gas velocities to entrain large amount of droplets, where Sterman and Panasenko correlations need much higher superficial gas velocities values.

The over prediction in Kataoka and Ishii’s correlation might also be related to the exponent in Eq. (II-9). The exponent of the ratio j^*/h^* is up to 20th power. In these conditions the entrainment might be affected by the Bernoulli effect when droplets pass through a break, as in the experiment conducted by Kim and No (2003). Kataoka and Ishii used data from different authors as mentioned earlier, under pressure from 1 bar to 185 bar. The over prediction could be also explained by the fact that the distance between the swell level and the entrainment measurement point is significantly small, allowing more droplet to be entrained even for smaller superficial gas velocities comparing to the present correlation under churn turbulent flow regime. Detailed review on the effect of the thermal hydraulics on bubble column could be found in (Ouallal, 2021).

The present correlation is empirical, which means its uncertainty is obtained from the experimental data. Most of the uncertainty of experimental data, that correspond to churn turbulent flow regime, used to develop this correlation are not available in the open literature. However, an uncertainty of a factor 2o 5 for bubbly and transition flow regime were obtained in the experiments of THAI (Freitag and Schmidt, 2017) (Table IV-2).

In this section, it was shows how the entrainment of water droplet is affected. The effect of the bubble dynamics in the pool by analysing the flow regime and the characteristics of the bubble size and their ability to produce droplets, either by the bubble burst in the bubble flow regime or the transition regime or by the shear of the water ligament in the churn turbulent flow regime was given. The effect of thermal-hydraulics such as the pressure has a slight effect on bubble size up to 16 bar and it was demonstrated experimentally by Cosandey (1999). In this range of pressure, the entrainment is affected but not noticeably, since the

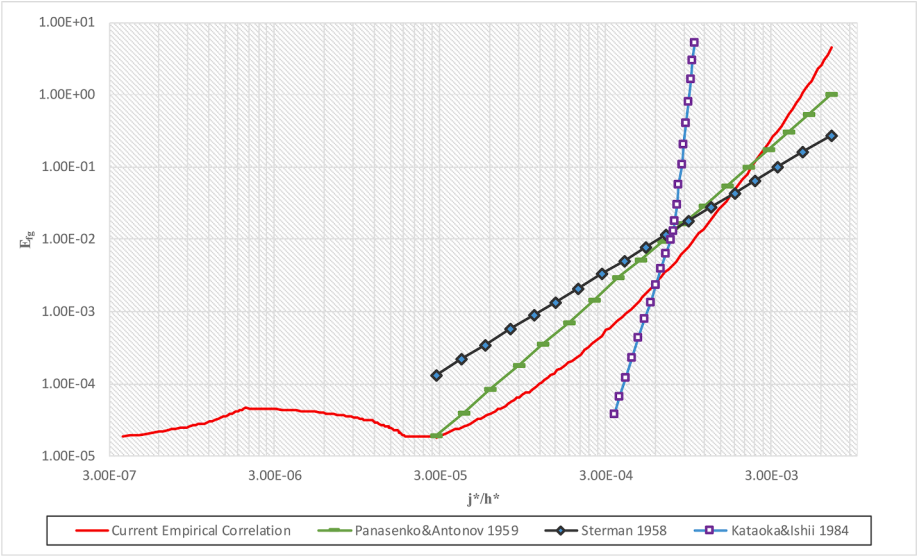

Fig. IV-3. Eqs. (III-1) to (III-3) as a function of ratio j*/h*).

change lies in the entrainment uncertainty. For extremely high pressure, up to 200 bar (Lin et al., 1998; Sterman et al., 1957), the entrainment is affected considerably since the bubble size decreasing with increasing the pressure further. As for the temperature, when it increases, the surface tension decrease, affecting bubble stability and their soon breakup (Poulain et al., 2018). Interestingly, the effect of temperature contributes in the aerosol agglomeration at the surface of the pool when increased. This effect of agglomeration has the ability to decrease the number of the produced droplet for bubble in the bubbly flow and transition regimes.

Droplet produced in the churn turbulent flow regime are more easily to retain than tiny droplet produced in bubbly flow regime (Dehbi et al., 2016).

5. Summary

An empirical correlation for droplet entrainment and carry over from a bubbling pool by gas have been developed using experimental data found in the open literature and from experimental programs. The analysis reveals that the entrainment could be evaluated in three flow regimes. In the range of superficial gas velocity [0, 0.05] m/s, the flow regime is attributed to bubbly flow regime; the bubbles could be assumed uniform in size, and the entrainment increase. In the transition regime, the range of superficial gas velocity is [0.05, 0.1] m/s, the bubbles follow a lognormal distribution, and the entrainment decrease slightly. When the superficial gas velocity increase further, the entrainment increase sharply and the flow regime is referred to churn turbulent. The correlation is a piecewise function as Eq. (V.1):

$$E_{fg} = \begin{cases} \gamma_1 . exp\left(\gamma_2 . \dfrac{j^*}{h^*}\right) & 0 \leqslant j_g \leqslant 0.05\ m/s \\ \gamma_3 . \dfrac{j^*}{h^*} + \gamma_4 & 0.05 m/s\ <\ j_g \leqslant 0.1\ m/s \\ \gamma_5 * \left(\dfrac{j^*}{h^*}\right)^{\gamma_6} & j_g > 0.1\ m/s \end{cases} \quad \text{(V-1)}$$

Despite the scatter of some experimental data for low superficial gas velocities, the comparison of Eq. (V.1) with a large number of data showed good agreement over the range of pressure [1, 16] bar, for containment applications. The bubble behaviour at the surface of the pool still needs further attention for their ability to generate droplets depending of bubble size and physical properties of the liquid phase. This correlation could be considered as a good candidate to be implemented in computer codes since it provides wide range of applicability.

CRediT authorship contribution statement

M. Ouallal: . **S. Leyer:** Supervision, Writing – review & editing. **S. Gupta:** Conceptualization, Formal analysis, Methodology, Supervision, Validation, Writing – review & editing.

Declaration of Competing Interest

The authors declare that they have no known competing financial interests or personal relationships that could have appeared to influence the work reported in this paper.

Acknowledgements

A special thanks to Dr. Pr. Abdel Dehbi from Paul Scherrer Institute (PSI), Switzerland for his assistance and fruitful discussions, which provided valuable insights in the studied phenomena.

Funding

This research did not receive any specific grant from funding agencies in the public, commercial, or not-for-profit sectors.

References

Akita, K., Yoshida, F., 1974. Bubble size, interfacial area, and liquid-phase mass transfer coefficient in bubble columns. Ind. Eng. Chem. Process Des. Dev. 13 (1), 84–91. https://doi.org/10.1021/i260049a016.

Andrews, J.M., 1960. Kinetic study of fluidized solids entrainment. Ind. Engr. Chem. 52 (1), 85–88.

Bagul, R.K., Pilkhwal, D.S., Vijayan, P.K., Joshi, J.B., 2019. Experimental investigations on carryover in a gravity separation-based steam drum. J. Nucl. Eng. Radiat. Sci. 5, 1–12. https://doi.org/10.1115/1.4041791.

Berzal, M.E., Espigares, M.M., Jimenez, J.L., Herranz, L.E., Peyrés, V., Polo, J., Kortz, C., Koch, M.K., Brockmeier, U., Unger, H., Dutton, L.M.C., Smedley, C., Trow, W., Jones, A.V., Bonanni, E., Calvo, M., Alonso, A., 1996. Pool scrubbing. Inf. Tec. Ciemat 805, 50.

Blanchard, D.C., 1989. The size and height to which jet drops are ejected from bursting bubbles in seawater. J. Geophys. Res. Ocean. 94 (C8), 10999. https://doi.org/10.1029/JC094iC08p10999.

Blanchard, D.C., Syzdek, L.D., 1988. Film drop production as a function of bubble size. J. Geophys. Res. 93 (C4), 3649. https://doi.org/10.1029/JC093iC04p03649.

Bunt, R., Corradini, M., Ellison, P., Farmer, M.., Francis, M., Gabor, J., Gauntt, R., Henry, C., Linthicum, R., Luangdilok, W., Lutz, R., Paik, C., Plys, M., Rabiti, C., 2015.

Reactor Safety Gap Evaluation of Accident Tolerant Components and Severe Accident Analysis. NURETH-16 4661–4674.
Bunz, H., Koyro, M., Propheter, B., Schoeck, W., Wagner - Ambs, M., 1992. Resuspension of fission products from sump water. 32.05.02; LK 01; EUR-Report 3009-86-07 EL ISP D.
Clift, R., Grace, J.R., Weber, M.E., 1978. Bubbles, Drops, and Particles. Acad. Press.
Colomer, A.G., Rogers, R.L., 2006. Evaluation of alternative swell models for reactor relief. Inst. Chem. Eng. Symp. Ser. 596–622.
Cosandey, J., 1999. Droplet production over a boiling pool during a slow depressurization. PhD thesis ETH Zürich, 179. 10.3929/ethz-a-010782581.
Cosandey, J.O., von Rohr, P.R., 2001. Entrainment of soluble and non soluble tracers from a boiling water surface. Nucl. Eng. Des. 208 (1), 87–97. https://doi.org/10.1016/S0029-5493(01)00354-5.
Dapper, M., 2009. Modellierung der nassen Resuspension und Analyse des Einflusses auf den Quellterm bei Kühlmittelverluststörfällen. Selbstverlag. des Lehrstuhls für Energiesysteme und Energiewirtschaft, Ruhr-Uni. 193.
Dehbi, A., Suckow, D., Lind, T., Guentay, S., Danner, S., Mukin, R., 2016. Key findings from the artist project on aerosol retention in a dry steam generator. Nucl. Eng. Technol. 48 (4), 870–880. https://doi.org/10.1016/j.net.2016.06.001.
Freitag, M., Schmidt, E., 2017. Re-Entrainment of Fission Products from Water Pools at Elevated Temperature. Tech. Rep. No. 150 1516 – TR – WH24.
Garner, F.H., Ellis, S.R.M., Lacey, J.A., 1954. The size distribution and entrainment of droplets. Trans. Inst. Chem. Eng 32, 222–235.
Golub, S.I., 1970. Investigation of moisture carryover and separation in evaporation apparatus, in: Candidates Dissertation. MEI.
Günther, A., Wälchli, S., von Rohr, P.R., 2003. Droplet production from disintegrating bubbles at water surfaces. Single vs. multiple bubbles. Int. J. Multiph. Flow 29 (5), 795–811. https://doi.org/10.1016/S0301-9322(03)00041-7.
Herranz, L.E., 2017. Pool Scrubbing in Severe Accident Sequences: Identification of Key Boundary Conditions. IPRESCA Kick off Meet.
Jamialahmadi, M., Muller-Steinhagen, H., 1990. Effect of electrolyte concentration on bubble size and gas hold-up in bubble columns. Chem. Eng. Res. Des. 68, 202–204.
Kataoka, I., Mamoru, I., 1983. Mechanistic Modeling and Correlations for Pool Entrainment Phenomenon. Nureg/Cr-3304 ANL-83-37.
Kharoua, N., Khezzar, L., Saadawi, H., 2013. CFD modelling of a horizontal three-phase separator: a population balance approach. Am. J. Fluid Dyn. 3, 101–118. https://doi.org/10.5923/j.ajfd.20130304.03.
Kim, C.H., No, H.C., 2005. Liquid entrainment and off-take through the break at the top of a vessel. Nucl. Eng. Des. 235 (16), 1675–1685. https://doi.org/10.1016/j.nucengdes.2005.01.014.
Kim, C.H., No, H.C., 2003. Liquid entrainment and off-take through the break at the top of a vessel. Trans. Am. Nucl. Soc. 89, 426.
Koch, M.K., Voßnacke, A., Starflinger, J., Schütz, W., Unger, H., 2000. Radionuclide re-entrainment at bubbling water pool surfaces. J. Aerosol Sci. 31 (9), 1015–1028.
Kolokoltzev, V.A., 1952. An Investigation of the Conditions in the Steam Space of ISV Evaporators. Diss. Transl, Power Inst, p. 10.
Kruzhilin, G.N., 1951. The dependence of the permissible vapor load upon the pressure. Izv. Akad. Nauk. Otd. Tekh. Nauk. 7, 1106.
Kudo, T., Yamano, N., Moriyama, K., Maruyama, Y., Sugimoto, J., 1994. Experimental Study of Aerosol Reentrainment Experimental Study of Aerosol Reentrainment From Flashing Pool in ALPHA Program, in: The Third International Conference on Containment Design and Operation, Toronto, Canada. Toronto, p. 11.
Lebel, L.S., Lessard, E., Batten, K., Clouthier, T., 2020. Experimental evaluation of re-entrainment from wet scrubber filtered containment venting systems. Nucl. Eng. Des. 369, 13. https://doi.org/10.1016/j.nucengdes.2020.110837.
Lhuissier, H., Villermaux, E., 2012. Bursting bubble aerosols. J. Fluid Mech. 696, 5–44. https://doi.org/10.1017/jfm.2011.418.
Lin, T.-J., Tsuchiya, K., Fan, L.-S., 1998. Bubble flow characteristics in bubble columns at elevated pressure and temperature. AIChE J. 44 (3), 545–560. https://doi.org/10.1002/(ISSN)1547-590510.1002/aic.v44:310.1002/aic.690440306.
Müller, M., von Rohr, P.R., 1997. Revent program – Modelling of aerosol reentrainment from boiling pool during controlled filtered venting after a severe core melt accident. J. Aerosol Sci. 28, S711–S712.
Ouallal, M., 2021. Entrainment of Droplets from Water Pools. University of Luxembourg.
Panasenko, M.D., Antonov, A.I., 1959. Correlation of mechanical carryover by steam. Teploenergetika 6.
Poulain, S., Villermaux, E., Bourouiba, L., 2018. Ageing and burst of surface bubbles. J. Fluid Mech. 851, 636–671. https://doi.org/10.1017/jfm.2018.471.
Reeks, M.W., Reed, J., Hall, D., 1988. On the resuspension of small particles by a turbulent flow. J. Phys. D Appl. 21 (4), 574–589.
Resch, F., Afeti, G., 1992. Submicron film drop production by bubbles in seawater. J. Geophys. Res. 97 (C3), 3679. https://doi.org/10.1029/91JC02961.
Rozen, A.M., Golub, S.I., Davydov, I.F., Gostinin, G.I., 1970. Some Laws Governing Drop Carry Over, in: Soviet Physics Doklady. p. 648.
Rozen, A.M., Golub, S.I., Votintseva, T.I., 1976a. On the nature of degree of dependence of transported carryover on vapor velocity with bubbling. Teploenergetika 23, 55.
Rozen, A.M., Golub, S.I., Votintseva, T.I., 1976b. Calculating droplet carryover with bubbling. Teploenergetika 23, 59.
Ruzicka, M.C., Zahradník, J., Drahoš, J., Thomas, N.H., 2001. Homogeneous-heterogeneous regime transition in bubble columns. Chem. Eng. Sci. 56 (15), 4609–4626. https://doi.org/10.1016/S0009-2509(01)00116-6.
de Santiago, M.R., 1991. Etude de l'entrainement de gouttelettes a la surface libre du liquide dans une colonne a bulles. PhD thesis. Univ. Joseph FOURIER.
de Santiago, M.R., Marvillet, C., 1991. Pool entrainment phenomenon: measurement of size and velocity distributions of droplets at several distances above the bubbling surface. Int. Commun. Heat Mass Transf. 3, 499–511.
Schmidt, E.W., Gupta, S., Freitag, M., Poss, G., Von Laufenberg, B., 2015. Wet resuspension of insoluble material from a boiling sump. Tech. Rep. No.1501361–TR–TH25.
Shah, Y.T., Kelkar, B.G., Godbole, S.P., Deckwer, W.-D., 1982. Design parameters estimations for bubble column reactors. AIChE J. 28 (3), 353–379. https://doi.org/10.1002/aic.690280302.
Spiel, D.E., 1998a. On the births of film drops from bubbles bursting on seawater surfaces smaller than their parents and which have upward velocity oscillation. J. Geophys. Res. 103 (C11), 24907–24918.
Spiel, D.E., 1998b. On the births of film drops from bubbles bursting on seawater surfaces. J. Geophys. Res. Ocean. 103 (C11), 24907–24918. https://doi.org/10.1029/98JC02233.
Sterman, L.S., 1958. On the theory of steam separation. Sov. Phys. Tech. Phys. 3, 1440–1451.
Sterman, L.S., 1952. Kotloturbostroenie. no. 5.
Sterman, L.S., Antonov, A.I., Surnov, A.V., 1957. An investigation of steam quatility at 185 atm. Teploenergetika 3, 17.
Sterman, L.S., Antonov, A.I., Surnov, A. V, 1958. An Investigation of the Steam Quality at 185 atm Using Radioactive Isotopes. Teploteh. i Gidrodynamika.
Styrikovich, M.A., Petukhov, V.I., Kolokoltsev, V, A., 1964. The effect of gas phases density on the extent of droplet entrainment. Teploenergetika 11.
Styrikovich, M.A., Sterman, L.S., Surnov, A.V., 1955. An investigation of the carry over of salt by steam using radioactive isotopes. Teploenergetika 2.
Viles, J.C., 1993. Predicting liquid re-entrainment in horizontal separators. JPT. J. Pet. Technol. 45, 405–409. https://doi.org/10.2118/25474-PA.
Wei, Y., Chen, H., Gu, H., Chen, L., Yu, X., 2020. Experimental investigation of the puncture position and film rolling speed of bubbles bursting under different liquid pool conditions. Prog. Nucl. Energy 129, 13. https://doi.org/10.1016/j.pnucene.2020.103510.
Wilkinson, Peter M., Dierendonck, Laurent L.V, 1990. Pressure and gas density effects on bubble break-up and gas hold-up in bubble columns. Chem. Eng. Sci. 45 (8), 2309–2315. https://doi.org/10.1016/0009-2509(90)80110-Z.
Wurster, S., Meyer, J., Kolb, H.E., Kasper, G., 2015. Bubbling vs. blow-off - On the relevant mechanism(s) of drop entrainment from oil mist filter media. Sep. Purif. Technol. 152, 70–79. https://doi.org/10.1016/j.seppur.2015.08.012.
Yeh, G., Zuber, N., 1960. On The Proplem of Liquid Entrainment. Report.
Zenz, F.A., Weil, N.A., 1958. A theoretical-empirical approach to the mechanism of particle entrainment from fluidized beds. AIChE J. 4 (4), 472–479. https://doi.org/10.1002/aic.690040417.
Zhang, Jiaqi, Chen, John J.J., Zhou, Naijun, 2012. Characteristics of jet droplet produced by bubble bursting on the free liquid surface. Chem. Eng. Sci. 68 (1), 151–156. https://doi.org/10.1016/j.ces.2011.09.019.
Zhang, P., Chen, P., Li, W., Di, Z., Zhang, L., Hu, X., Zou, Y., 2016. An experimental study of pool entrainment in high gas flux region. Prog. Nucl. Energy 89, 191–196. https://doi.org/10.1016/j.pnucene.2016.02.017.